ACS OMEGA

http://pubs.acs.org/journal/acsodf

Article

Study on the Effective Well Depth of Single U-Shaped Vertical Buried Pipes Based on Temperature Difference Analysis

Rui Zhang* and Yanping Xin

Cite This: *ACS Omega* 2023, 8, 24964−24979

Read Online

ACCESS | Metrics & More | Article Recommendations

ABSTRACT: A heat transfer model of a single U-shaped vertical buried pipe similar to an actual scenario is established, and the accuracy of the model is verified by experiments. The model is used to analyze the heat transfer performance of vertical buried pipe heat exchangers with well depths of 200, 160, 120, and 80 m. This includes the heat transfer per unit well depth, temperature change of the well wall and fluid along the pipe length, heat transfer coefficient, and section heat transfer validity. With the increase in well depth, the heat exchange per unit well depth decreases, and the proportion of heat exchange in the inlet section to the total heat exchange increases. When the well depths are 200, 160, 120, and 80 m, the last 10 m pipe sections have 30, 40.3, 53.7, and 66.4% of the heat exchange efficiencies of the initial 10 m pipe section, respectively. To obtain a reasonably effective well depth of a single U-shaped vertical buried pipe, it is necessary to comprehensively consider the heat exchange per unit well depth, the temperature difference between the well wall and the fluid, and the energy efficiency of the buried pipe section. Moreover, it should be analyzed in combination with economic factors.

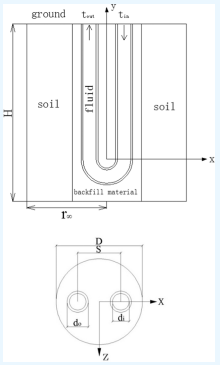

1. INTRODUCTION

A ground source heat pump system is a type of cold and heat source using shallow geothermal resources, which has significant energy-saving benefits. Ground source heat pump systems with buried pipes are commonly used, and their heat exchange performance is the main factor determining their operation efficiency.[1]

Researchers worldwide have conducted a considerable number of studies on the performance of buried tube heat exchangers. Yu et al. established a layered soil-buried pipe heat transfer model of a column heat source and verified the accuracy of the model by conducting layered geotechnical thermal response tests. Moreover, they compared and analyzed the heat transfer characteristics of the buried pipe heat exchanger under different working conditions using a homogeneous soil model.[2] Min further studied the heat transfer process of single and double U-shaped buried pipe systems and the surrounding soil system by building a test bed and establishing a numerical model of the vertical buried pipes.[3] Chwieduk proposed a new numerical model of a vertical U-tube buried tube heat exchanger (GHE) to conduct a highly accurate, detailed, and reasonable rapid simulation of the GHE system to ensure reasonable selection of the GHE in the design process.[4] On the premise of considering the vertical temperature gradients of the rock and soil, Lu simulated and calculated the influencing factors of a single U-shaped buried pipe heat exchanger: inlet and outlet water temperatures, rock and soil temperatures, and heat exchange per unit drilling depth.[5] Chen established a finite line heat source model of a buried tube heat exchanger and analyzed its temperature change and heat exchange per unit length. By conducting computational fluid dynamics simulations, the heat transfer characteristics of four single U-shaped buried tube heat exchanger combinations were analyzed, the temperature field distributions of the heat exchangers and soil were obtained, and the temperature recovery characteristics of the soil were studied.[6] Xu et al. summarized the research on ground pipe heat exchangers of ground source heat pumps and discussed the research status and development trend of ground pipe heat exchangers. They also analyzed the main factors affecting the heat exchange of a ground pipe heat exchanger and the measures to enhance its heat exchange.[7] To improve the uniformity of the underground temperature field after using a ground source heat pump system in areas with unbalanced cooling and heating loads, Guo et al. used an underground pipe group composed of 36 boreholes, a cooling and heating load ratio of 2.5:1.0, and an operation period of 20 years as an example. Accordingly, they proposed three zoning optimized buried pipe layout methods with a dense outside and a sparse inside.[8] To study the effects of different thermophysical properties of layered geotechnical layers on the overall heat transfer efficiency of a pipe group, Jin and Li used the finite-length linear heat source theory. Moreover, considering the geotechnical stratification phenomenon and pipe group conditions, they established and verified

Received: March 7, 2023
Accepted: June 13, 2023
Published: July 7, 2023

https://doi.org/10.1021/acsomega.3c01207
ACS Omega 2023, 8, 24964−24979

the layered heat transfer analytical model of the pipe group. They also introduced a dimensionless number reflecting the regional heat efficiency as the evaluation index of the heat transfer characteristics of the pipe group.[1] He used the adaptive load method to analyze the heat transfer of a buried pipe and the inlet water temperature and soil temperature distributions during long-term operation of the buried pipe heat exchanger. Moreover, he compared his method with the commonly used load sharing method.[9] Cai and others studied and analyzed the factors affecting the heat exchange capacity of a vertical buried pipe heat exchanger from the perspective of engineering practice and classified them into three categories: geological, engineering, and operation factors. The considered factors were the initial average temperatures of the rock and the soil, the geological structure, the thermophysical properties of the rock and the soil, hydrogeological conditions, depth of the heat source hole, type of heat exchanger, backfill material, flow rate of the heat exchange medium, and operation mode.[10] To explore the influence of phase change on the thermal response characteristics of a phase change material (PCM)-backfilled buried tube heat exchanger, Yang et al. established its phase change heat transfer mathematical model and numerically solved it using FLUENT software. Furthermore, they analyzed the effects of the phase change process and the PCM physical parameters on the diffusion and recovery mechanism of the soil temperature around the buried tube heat exchanger.[11] Shang et al. studied the variation law of the soil temperature around the ground pipe heat exchanger of a ground source heat pump with different soil-specific heat capacities.[12] Wang et al. proposed a rectangular straight-rib buried tube heat exchanger and established its underground heat transfer model. They also simulated and analyzed the effects of the structural and operating parameters of the straight-rib buried pipe on the heat transfer performance of single and double U-type buried pipe heat exchangers using MATLAB software.[13] Bao and others analyzed the underground heat transfer principle of a vertical buried pipe heat exchanger in combination with the characteristics of the climate temperature, geological structure, and soil thermophysical properties in Wuhan and established a vertical double U-shaped buried pipe heat transfer model. They conducted numerical simulation calculations under summer working conditions using ANSYS CFX software to obtain the distribution of the temperature field of the buried pipe and its surrounding soil and the change in the temperature field with time. It was considered that the distributions of the temperature field around the inlet and outlet of a vertical double U-shaped buried pipe are lagging.[14] Tang et al. conducted continuous tests of the operating parameters of ground source heat pump systems in six actual offices, hospitals, and residential buildings in Nanjing during summer and winter. They analyzed and evaluated the outlet water temperature and heat transfer resistance of the buried pipes.[15]

With increasing maturity of the construction technology of buried pipes, the buried depths of vertical buried pipes also increase, and they are generally 40−200 m.[16] An increase in the buried pipe depth can effectively save the floor area; however, simultaneously, it increases the construction cost, thereby reducing the heat exchange per unit well depth.[17]

Some studies have also examined the influence of the buried pipe depth on the performance of a heat exchanger. Cai and others conducted winter working condition experiments using a ground source heat pump experimental device with a vertical tube heat exchanger under different buried depths built in Songjiang District, Shanghai. They tested the heat exchange of the outdoor heat exchanger during heat pump operation and obtained the key parameter of the heat exchange per unit well depth.[18] Based on the unbalance coefficient, Jin et al. studied the influence of the buried depth on the thermal short circuit between inlet and outlet pipes and concluded that the thermal short circuit unbalance coefficient of buried pipes increases with the increase in buried depth.[19] Li et al. studied the influence of buried pipe depth and the connection length between two vertical pipes on the buried pipe heat transfer.[20] By numerical simulation, Li and others studied the effects of changing the aquifer thickness, groundwater seepage velocity, and groundwater level on the heat transfer performance of buried pipes. Finally, they proposed a method to determine the optimal buried depth of buried pipes based on the thickness of typical aquifers.[21] Lin et al. studied the heat exchange performance of a vertical buried tube heat exchanger and found that it presents three heat exchange sections with different characteristics with the change in buried depth and that thermal short circuit and thermal accumulation occur in the near section. They proposed an optimization method of taking the cutoff depth of the high-efficiency section of the heat exchange as the buried depth of the vertical buried tube heat exchanger.[22] On a project site at Xuzhou, Li and others analyzed the heat exchange characteristics of buried pipes in a layered geological structure and proposed that the buried depths of buried pipes should be guided by considering the stratum structure. Moreover, they studied the variation law of the inlet water temperature, circulating water flow rate, operation mode, and layered heat exchange.[23] Deng et al. conducted on-site thermal response experimental research on the common diameter and depth of a buried pipe heat exchanger in a ground source heat pump system in a loess area. They concluded that the depth of a double U32 pipe is no more than 120 m; therefore, it should be the preferred heat exchanger in a loess area, which can provide reference for ground source heat pump projects of other similar geomorphic units.[24] Yang et al. established a three-dimensional model and studied the effects of fluid velocity and buried depth on heat transfer in a vertical U-tube underground heat exchanger based on fluid structure coupling simulation.[25] Changxing et al. proposed a simple mean fluid temperature analysis method for calculating borehole thermal resistance. They further investigated the influence of borehole depth and volume flow on the root-mean-square error distribution of borehole thermal resistance and effective borehole thermal resistance.[26] Shangyuan et al. developed an artificial neural network model that can predict the depth of a vertical GHE according to the given design parameters. Specifically, the soil thermal conductivity, grouting thermal conductivity, inflow flow, inflow temperature, groundwater velocity, and heat flux density are input parameters, and the borehole depth is the output parameter.[27] Wei et al. analyzed the effects of porosity and the temperature field on a settlement and discussed the optimal buried depth of a U-shaped pipe under a foundation.[28]

In addition, some scholars have studied the comprehensive heat transfer coefficient of a heat exchanger. Honda et al. developed an empirical equation for the superficial vapor phase heat transfer coefficient on the basis of the analogy between heat and mass transfer.[29] Koji et al. presented the results of an experimental investigation into the water boiling heat transfer in a minichannel conduit vertically oriented with an upward flow.[30]

A modified surface and a bionic structure are widely applied to heat pipes. Cong et al. discussed the effects of two kinds of base

https://doi.org/10.1021/acsomega.3c01207
ACS Omega 2023, 8, 24964−24979

fluids (H_2O and Ga) and three different nanoparticle radiuses on the natural convection heat transfer of a rectangular enclosure filled with Al_2O_3−H_2O and Al_2O_3−Ga nanofluids at different Rayleigh numbers based on a two-phase lattice Boltzmann method.[31] Wang et al. used a silica−water (SiO_2−H_2O) nanofluid as a working medium and researched the effects of tube structure, twisted tape hole spacing, and hole shape on the flow and heat exchange characteristics of nanofluids in the tube by numerical simulation.[32] Jianglin et al. analyzed the effects of micro-rib structure types, number of ribs, height of ribs, pitch diameter ratio, mass fractions, and Reynolds numbers on the flow and heat transfer characteristics of tube-row channel heat exchangers.[33] Chengchao et al. constructed a physical model of a heat pipe with an ordinary and modified surface to numerically simulate the thermal performance inside the heat pipe.[34] Kazemi−Beydokhti et al. researched the role of new nanofluids based on multiwalled carbon nanotubes (MWCNTs) on the heat transfer efficiency of a closed-loop pulsating heat pipe (CLPHP).[35] Leu et al. aimed to measure the heat transfer performance in a heat pipe cooling device under a constant heat flux condition. Emphasis is placed on the surface modification of heat pipes to enhance the heat transfer performance.[36]

Taking the working condition in summer as an example, when the fluid flows in a buried pipe heat exchanger, it transfers heat to the soil through its pipe wall and backfill material. As the fluid temperature decreases, the temperature difference between the fluid and the soil increasingly reduces, and the heat exchange capacity decreases. Therefore, a very deep buried pipe is ineffective. In this study, a three-dimensional model of a single U-shaped vertical buried pipe is established. Based on the difference between the wellbore and fluid temperatures, the heat transfer of the buried pipe heat exchanger is analyzed from the perspective of effective heat transfer, to study the effective well depth.

2. ESTABLISHMENT AND VERIFICATION OF A SINGLE U-SHAPED BURIED PIPE MODEL

2.1. Physical Model. In a common single U-shaped vertical buried pipe heat exchanger, a U-shaped pipe is inserted into a drilling well, and the well is sealed with a backfill material to form a complete structure with the surrounding soil, as shown in Figure 1. During the operation of the buried pipe heat exchanger system, the U-shaped pipe is divided into inlet and outlet sections according to the flow direction of the fluid. The fluid flows from the inlet section of the U-shaped pipe to the bottom of the borehole and subsequently flows out from the outlet section to realize heat exchange between the fluid in the pipe and the surrounding soil.

2.2. Mathematical Model. *2.2.1. Establishment of Governing Equations.* (1) Governing equation of thermal conductivity of the surrounding soil

$$\frac{\partial t_s}{\partial \tau} = \alpha_s\left(\frac{\partial^2 t_s}{\partial x^2} + \frac{\partial^2 t_s}{\partial y^2} + \frac{\partial^2 t_s}{\partial z^2}\right) \quad (1)$$

(2) Governing equation of thermal conductivity of the backfill material

$$\frac{\partial t_b}{\partial \tau} = \alpha_b\left(\frac{\partial^2 t_b}{\partial x^2} + \frac{\partial^2 t_b}{\partial y^2} + \frac{\partial^2 t_b}{\partial z^2}\right) \quad (2)$$

(3) Governing equation of heat conduction of the pipe wall

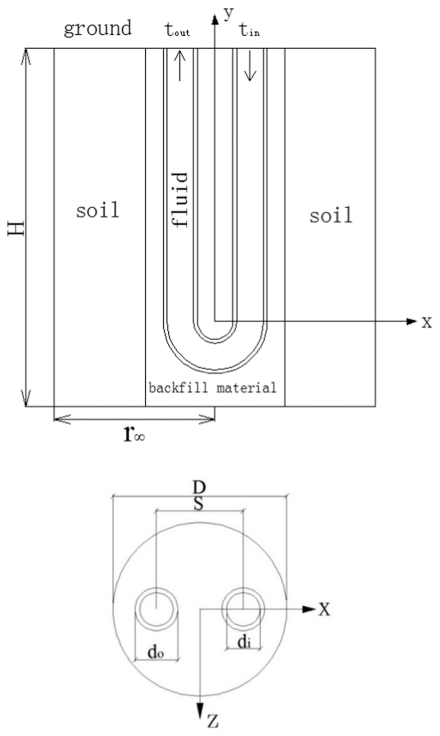

Figure 1. Schematic of a vertical single U-shaped buried pipe heat exchanger.

$$\frac{\partial t_p}{\partial \tau} = \alpha_p\left(\frac{\partial^2 t_p}{\partial x^2} + \frac{\partial^2 t_p}{\partial y^2} + \frac{\partial^2 t_p}{\partial z^2}\right) \quad (3)$$

(4) Governing equation of fluid in the pipe

(A) When the heat pump is running, the fluid performs convective heat transfer with the inner pipe wall.

i. Turbulence model: A model with a swirl correction (realizable model) is adopted, and the model equations are as follows:

$$\frac{\partial}{\partial t}(\rho k) + \frac{\partial}{\partial x_i}(\rho k u_j) = \frac{\partial}{\partial x_i}\left[\left(\mu + \frac{\mu_t}{\sigma_k}\right)\frac{\partial k}{\partial x_j}\right] + G_k + G_b - \rho\varepsilon - Y_M + S_k \quad (4)$$

$$\frac{\partial}{\partial t}(\rho \varepsilon) + \frac{\partial}{\partial x_j}(\rho \varepsilon u_j) = \frac{\partial}{\partial x_j}\left[\left(\mu + \frac{\mu_t}{\sigma_\varepsilon}\right)\frac{\partial \varepsilon}{\partial x_j}\right] + \rho C_1 S_\varepsilon - C_2\rho\frac{\varepsilon^2}{k + \sqrt{\nu\varepsilon}} + C_{1\varepsilon}\frac{\varepsilon}{k}C_{3\varepsilon}G_b) + S_\varepsilon \quad (5)$$

$$C = \max\left(0.43, \frac{\eta}{\eta + 5}\right), \quad \eta = S\frac{k}{\varepsilon}$$

$$\text{Turbulent viscosity:} \quad \mu_t = \rho C_\mu \frac{k^2}{\varepsilon}$$

$$\text{Model constant:} \quad C_\mu = \frac{1}{A_0 + A_s U^* k/\varepsilon}$$

where

https://doi.org/10.1021/acsomega.3c01207
ACS Omega 2023, 8, 24964−24979

$$U \equiv \sqrt{S_{ij}S_{ij} + \Omega_{ij}\hat{\Omega}_{ij}}, \quad \hat{\Omega}_{ij} = \Omega_{ij} - 2\varepsilon_{ijk}\omega_k,$$
$$\Omega_{ij} = \bar{\Omega}_{ij} - \varepsilon_{ijk}\omega_k, \quad A_0 = 4.04, \quad A_s = \sqrt{6}\cos\phi,$$
$$\phi = \frac{1}{3}\cos^{-1}(\sqrt{6}W), \quad W = \frac{S_{ij}S_{jk}S_{kj}}{\hat{S}}, \quad \hat{S} = \sqrt{S_{ij}S_{ij}},$$
$$S_{ij} = \frac{1}{2}\left(\frac{\partial u_j}{\partial x_i} + \frac{\partial u_i}{\partial x_j}\right)$$

Model constants C_2, σ_k, and σ_ε are optimized for a specification flow as follows:

$$C_{1\varepsilon} = 1.44,\ C_2 = 2,\ \sigma_k = 1.0,\ \sigma_\varepsilon = 1.2$$

ii. Continuity equation: $\frac{\partial u_x}{\partial x} + \frac{\partial u_y}{\partial y} + \frac{\partial u_z}{\partial z}$

iii. Momentum equation:

$$\rho\left(\frac{\partial u_x}{\partial \tau} + u_x\frac{\partial u_x}{\partial x} + u_y\frac{\partial u_x}{\partial y} + u_z\frac{\partial u_x}{\partial z}\right) = X - \frac{\partial p}{\partial x} + \mu\left(\frac{\partial^2 u_x}{\partial x^2} + \frac{\partial^2 u_x}{\partial y^2} + \frac{\partial^2 u_x}{\partial z^2}\right)$$
$$\rho\left(\frac{\partial u_y}{\partial \tau} + u_x\frac{\partial u_y}{\partial x} + u_y\frac{\partial u_y}{\partial y} + u_z\frac{\partial u_y}{\partial z}\right) = Y - \frac{\partial p}{\partial y} + \mu\left(\frac{\partial^2 u_y}{\partial x^2} + \frac{\partial^2 u_y}{\partial y^2} + \frac{\partial^2 u_y}{\partial z^2}\right)$$
$$\rho\left(\frac{\partial u_z}{\partial \tau} + u_x\frac{\partial u_z}{\partial x} + u_y\frac{\partial u_z}{\partial y} + u_z\frac{\partial u_z}{\partial z}\right) = Z - \frac{\partial p}{\partial x} + \mu\left(\frac{\partial^2 u_z}{\partial x^2} + \frac{\partial^2 u_z}{\partial y^2} + \frac{\partial^2 u_z}{\partial z^2}\right) \quad (6)$$

iv. Energy equation:

$$\frac{\partial t_f}{\partial \tau} + u_x\frac{\partial t_f}{\partial x} + u_y\frac{\partial t_f}{\partial y} + u_z\frac{\partial t_f}{\partial z} = \alpha_f\left(\frac{\partial^2 t_f}{\partial x^2} + \frac{\partial^2 t_f}{\partial y^2} + \frac{\partial^2 t_f}{\partial z^2}\right) \quad (7)$$

(B) When the heat pump is not operating, the fluid in the pipe is static, and the heat transfer between the fluid and the pipe wall is mainly in the form of heat conduction, which is expressed as

$$\frac{\partial t_f}{\partial \tau} = \alpha_f\left(\frac{\partial^2 t_f}{\partial x^2} + \frac{\partial^2 t_f}{\partial y^2} + \frac{\partial^2 t_f}{\partial z^2}\right) \quad (8)$$

In the above formulas, subscripts s, b, p, and f represent soil, backfill material, pipe wall, and fluid, respectively; α is the thermal conductivity, m^2/s, $\alpha = \frac{\lambda}{\rho c_p}$; λ is the thermal conductivity, W/(mK); ρ is the density, kg/m^3; c_p is the specific heat capacity, J/(kg°C); and t and u represent the temperature and the speed, respectively.

2.2.2. Geometric Condition. As shown in Figure 1, D is the diameter of the borehole, H is the depth of the borehole, d_i and d_o are the inside and outside diameters, respectively, S is the center distance between the two branches of the U-shaped pipe, and r_∞ is the radius of the far boundary. The settings of geometric parameters are shown in Table 1.

2.2.3. Initial Condition. The soil temperature at the far boundary is t_∞ and the initial temperature of the soil and the backfill material is t_0, when $\tau = 0$, $t_s = t_b = t_\infty = t_0 = 17.8$ °C (Shang Hai).

2.2.4. Boundary Condition.

Table 1. Geometrical Dimensions of the Buried Pipe Heat Exchanger

name	parameter (mm)	name	parameter (mm)
inside diameter of the U-shaped pipe d_i	25	depth of the borehole H	80,000
outside diameter of the U-shaped pipe d_o	32	diameter of the borehole D	130
center distance between the two branches of the U-shaped pipe S	65	radius of the far boundary r_∞	4000

(1) Ground surface.

Usually, the actual U-shaped pipe is buried 2 m below the ground, so the top surface in the model is actually 2 m below the ground. The heat transfer boundary condition is to conduct heat conduction with 2 m thick soil and then convective heat transfer with the outside air.

According to calculations, the convective heat transfer coefficient is 13.9 W/ (m^2 °C) in summer and 15.1 W/ (m^2 °C) in winter in Shanghai.

(2) Far boundary and bottom

The isothermal boundary conditions were taken for the far boundary and bottom, and the temperature was the initial temperature of the soil, namely, t_{bottom} = 17.8 °C, $t_{far\text{-}end}$ = 17.8 °C.

(3) Inlet fluid

Inlet boundary conditions include the inlet temperature, velocity, turbulence intensity, and hydraulic diameter. The temperature of the inlet fluid t_{in} is determined by the actual evaporator or condenser outlet temperature of the heat pump unit. Taking into account the heat transfer capacity and the circulating pump power consumption, the recommended flow rate of the buried tube heat exchanger is 0.4−0.6 m/s (this paper takes 0.6 m/s). Hydraulic diameter is the inner diameter of the round pipe. By calculation, when the inner diameter of the U-shaped tube is 25 mm, the turbulence intensity is 0.047 in summer and 0.05 in winter.

(4) Outlet fluid

The outlet boundary is defined as the pressure outlet. Using pressure outlet boundary conditions instead of mass outlet boundary conditions often results in better convergence rates when backflow occurs.

(5) Each contact wall surface.

The interface of the U-shaped water, U-shaped pipe, backfill material, and soil does not belong to any of the three boundary conditions. The temperature distribution of the boundary, the heat flux, and the relationship between them cannot be known in advance. They interact with each other. Both the wall temperature and the heat flux are part of the calculated results, not known conditions, and such boundaries are called coupled heat transfer boundaries.

2.3. Grid Division and Numerical Calculation.

2.3.1. Grid Division. A quadrilateral unstructured grid (quad/pave) is adopted for the inlet and outlet sections of the U-shaped pipe, and a quadrilateral structured grid (quad/map) is arranged for the section of the pipe wall. A quadrilateral unstructured grid (quad/pave) is adopted for the backfill material around the U-shaped pipe owing to its irregular shape. The grid of the soil around the borehole is relatively dense near the borehole and becomes sparse with the increase in distance from the borehole. Figure 2 shows the grid division of the backfill material and inlet

https://doi.org/10.1021/acsomega.3c01207
ACS Omega 2023, 8, 24964−24979

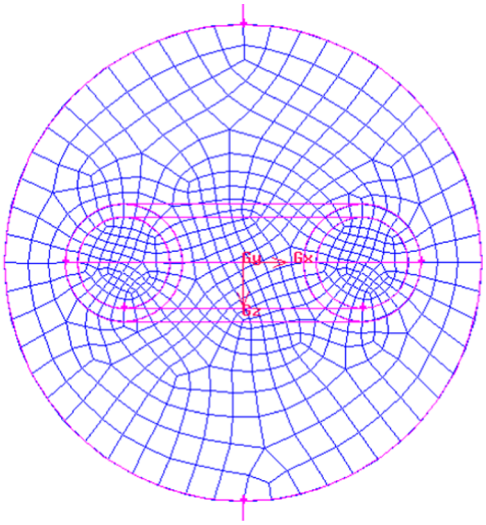

Figure 2. Grid division of the backfill material and inlet and outlet sections.

and outlet sections, and Figure 3 shows the grid division of the soil sections. Figure 4 shows the grid division of the U-bend and

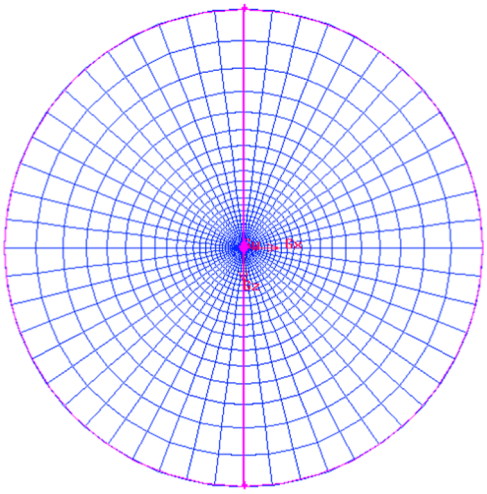

Figure 3. Grid division of the soil section around the single U-shaped pipe.

the surrounding backfill material. Figure 5 shows the grid division of the entire system.

2.3.2. Grid Independence Verification. Grid independence verification is carried out for the model with a depth of 80 m. This paper focuses on the heat transfer performance between the fluid in the pipe and the surrounding soil, which is closely related to the outlet temperature of the U-shaped pipe. Therefore, the outlet temperature of the U-shaped pipe during 24 h operation is selected as the parameter for grid independence verification, as shown in Figure 6. As can be seen from the figure, when the number of grids exceeds about 1,700,000, the water outlet temperature basically remains stable. In order to improve the calculation efficiency, ensure the calculation accuracy, and reduce the calculation error, the number of grids in the model is determined as 1,701,000.

2.4. Experimental Verification of the Model. The above model is verified using the summer experimental data of the ground source heat pump system experimental station of Tongji

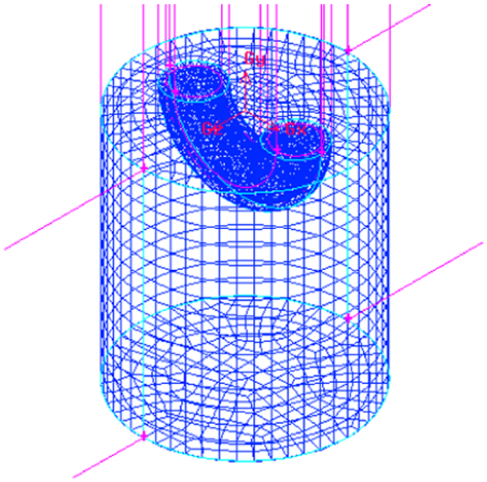

Figure 4. Grid division of the U-bend and the surrounding backfill material.

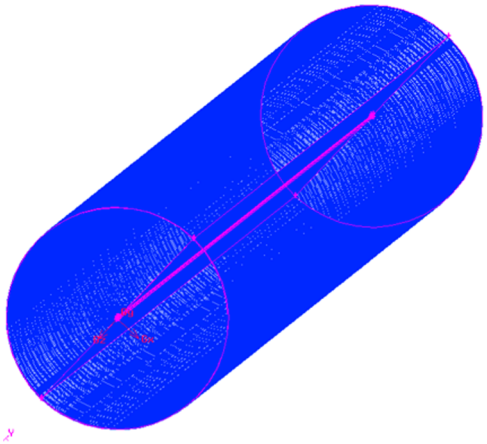

Figure 5. Grid division of the entire system.

University. In the experiment, the flow rate is constant, whereas the inlet water temperature changes with time. The average value is taken as the simulated boundary condition. The specific boundary condition settings are listed in Table 2.

Figure 7 shows the comparison of the simulated and experimental values of the heat exchange per unit well depth. During the simulation, it is assumed that the inlet water temperature remains unchanged and the heat exchange per unit well depth gradually decreases with the operation time. The actual heat exchange fluctuates with the change in the indoor cooling load; however, overall, it shows an attenuation trend, which is the same as the simulation results, and the attenuation becomes increasingly gradual. It can be seen from the simulation results that the initial 2 h of operation are unstable. After 2 h, the average heat exchange per unit well depth is 88.6 W/m, and the actual 24 h average heat exchange per unit well depth is 92.3 W/m. The comparison error between the simulation and experimental results is 3.9%, which is less than 10%, i.e., it is within a reasonable range.

Figure 8 shows the variation of the error between the experimental average value and the simulated value of heat exchange per unit well depth over time. It can be seen that the error between the simulated value and the experimental average value is large at the initial stage of the simulation operation, and

https://doi.org/10.1021/acsomega.3c01207
ACS Omega 2023, 8, 24964−24979

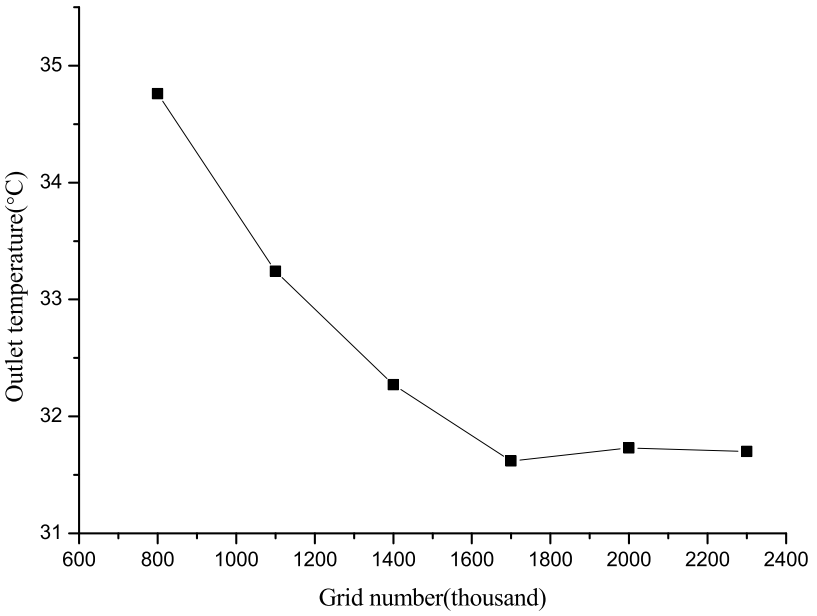

Figure 6. Grid independence verification diagram.

Table 2. Boundary Condition Setting of the Experimental Verification Model

working condition	average inlet water temperature (°C)	current speed (m/s)	running time (h)
case 1	45	0.3	24

the operation gradually tends to be stable after 5 h, with the error between them within ±15%.

In Figure 9, the experimental and simulated values of the borehole wall temperature of buried pipes at different depths are compared. Initially, the borehole wall temperature shows a rapid upward trend. The simulation results show that the rising speed of the borehole wall temperature gradually decreases after 2 h. The actual borehole wall temperature is affected by the inlet water temperature, which changes with the indoor load; therefore, the borehole wall temperature presents a fluctuating upward trend and sometimes slightly decreases. However, there is still a large temperature rise compared to the initial temperature. After 24 h of operation, the simulated value at 10 m depth is 34.33 °C, the experimental value is 36.23 °C, and the error is 5.2%. The simulated value at 30 m depth is 33.44 °C, the experimental value is 35.84 °C, and the error is 6.7%. The simulated value at 50m depth is 32.67 °C, the experimental value is 33.24 °C, the error is 1.7%. And all the errors are less than 10%, which are within a reasonable range.

3. COMPARISON OF THE HEAT TRANSFER PERFORMANCE OF BURIED PIPES AT DIFFERENT WELL DEPTHS

In this section, the analysis and comparison of single U-shaped buried pipe heat exchangers with well depths of 200, 160, 120, and 80 m are presented. Excluding the well depth, other geometric and boundary conditions are the same under the four

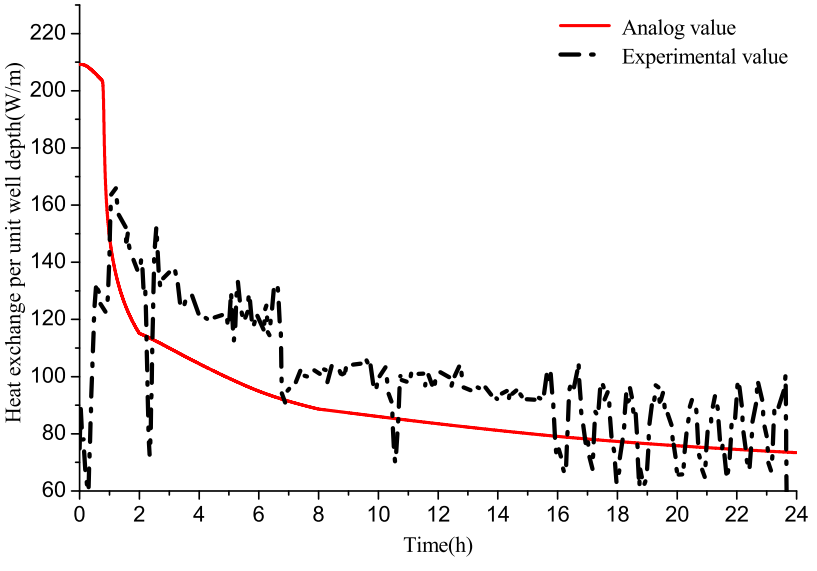

Figure 7. Comparison of experimental and simulated values of heat transfer per unit well depth of the buried pipe.

https://doi.org/10.1021/acsomega.3c01207
ACS Omega 2023, 8, 24964−24979

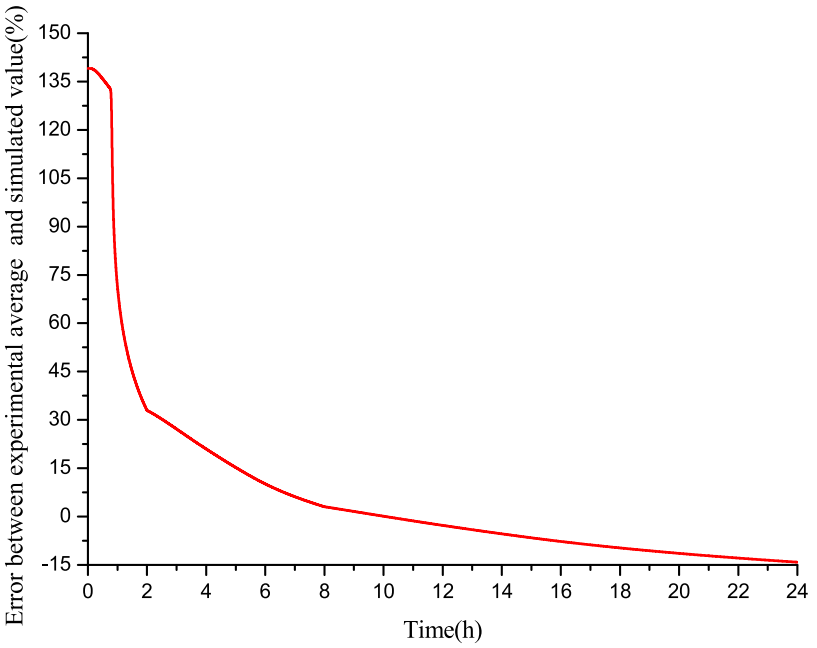

Figure 8. Error between the mean variation of experimental values and the simulated values of heat exchange per unit well depth.

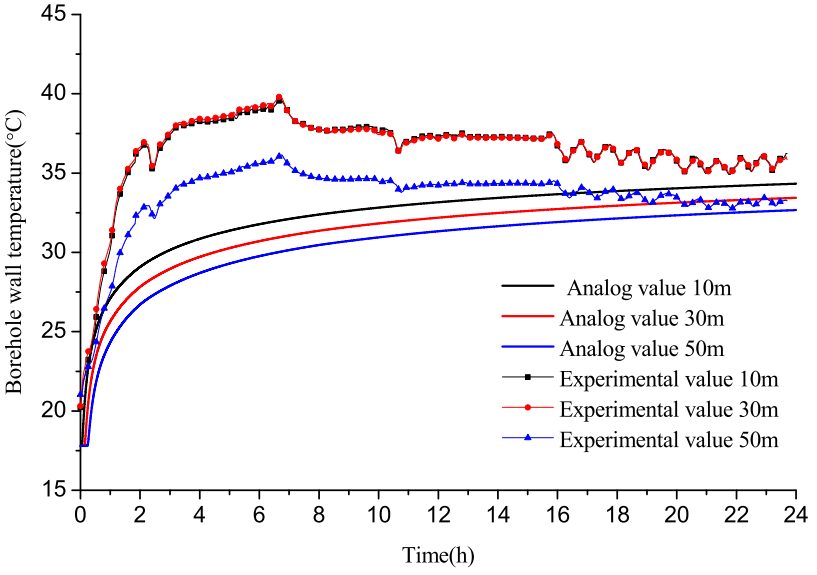

Figure 9. Comparison of experimental and simulated values of borehole wall temperature of buried pipes at different depths.

Table 3. Simulation Conditions for Different Well Depths

working condition	season	well depth (m)	inlet water temperature (°C)	current speed (m/s)	operation strategy	initial soil temperature (°C)
case 1	summer	200	35	0.6	continuous operation for 24 h	17.8
case 2		160				
case 3		120				
case 4		80				

working conditions, and FLUENT software is used for the numerical calculations. The specific simulation conditions are listed in Table 3.

3.1. Comparison of Heat Exchange per Unit Well Depth. Figure 10 shows the comparison of the heat exchange per unit well depth and the inlet and outlet water temperature differences during continuous operation for 24 h under summer conditions when the well depths are 200, 160, 120, and 80 m. It can be seen that a large well depth implies a large inlet and outlet water temperature difference but a small heat exchange per unit well depth. This is because a large well depth implies a long duration in which the fluid remains in the pipe, a low outlet water temperature, a large total heat exchange, and a low average temperature of the fluid. The temperature difference with the surrounding soil decreases, and the increased pipe length reduces the heat exchange per unit well depth owing to the

https://doi.org/10.1021/acsomega.3c01207
ACS Omega 2023, 8, 24964−24979

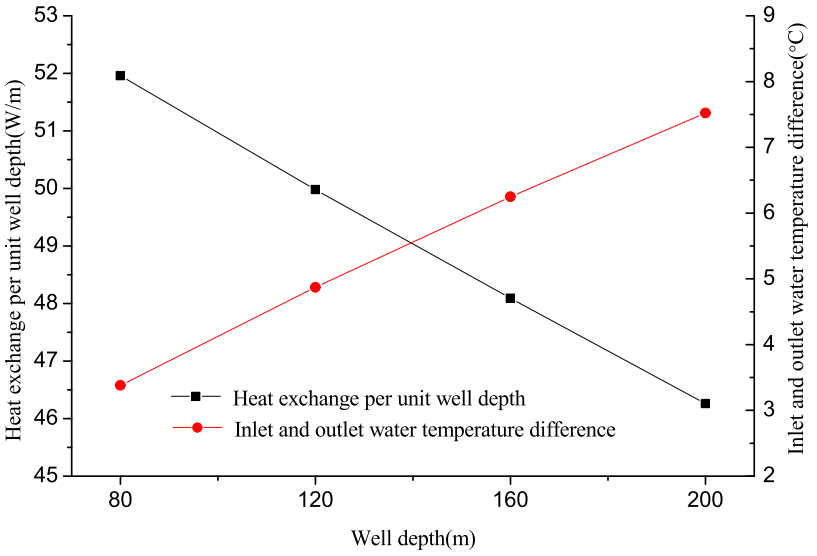

Figure 10. Comparison of heat exchanges per unit well depth and inlet and outlet water temperature differences during 24 h operation of buried pipes for different buried depths in summer.

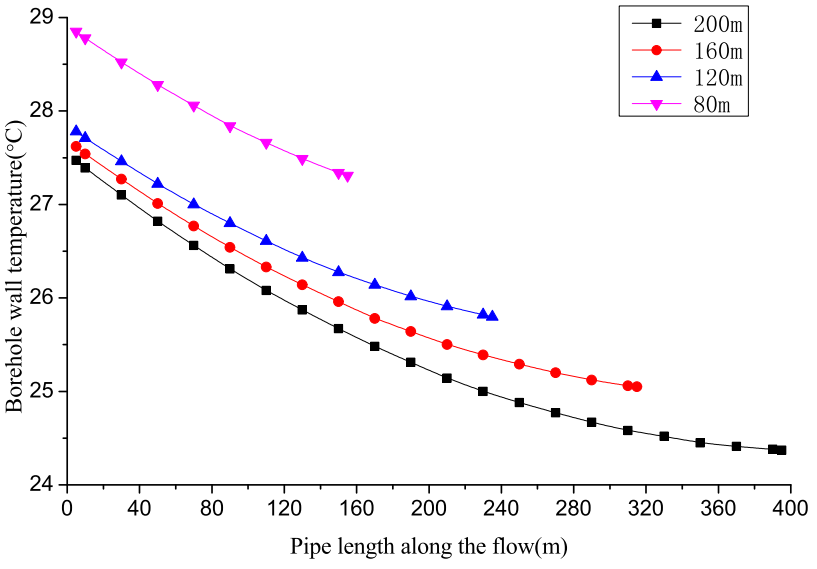

Figure 11. Borehole wall temperature distributions along the water flow direction after 24 h operation of buried pipes with different buried depths in summer.

decrease in the fluid temperature in the pipe. When the well depths are 200, 160, 120, and 80 m, the inlet and outlet water temperature differences are 7.52, 6.25, 4.87, and 3.38 °C, respectively. The corresponding heat exchanges per unit well depth are 46.26, 48.09, 49.98, and 51.96 W/m. When the well depth was 200 m, the inlet and outlet water temperature difference was 7.52 °C, which is 2.2 times that at 80 m, and the heat exchange per unit well depth was 46.26 W/m, which is 11% lower than that at 80 m. Increasing the well depth can increase the temperature difference between the inlet and outlet of the buried pipe and improve the total heat exchange; however, the heat exchange per unit well depth decreases. This suggests that a large well depth is effective.

3.2. Comparison of Wellbore and Fluid Temperatures in a U-Shaped Pipe. Figure 11 shows the distributions of the well wall temperature along the water flow direction when the well depths are 200, 160, 120, and 80 m in summer. It can be seen that a large well depth implies a low well wall temperature, and the well wall temperature decreases gradually along the water flow direction, with an increasingly reduced decreasing rate. When the well depth is 200 m, the temperature change from 5 to 50 m is 0.65 °C and that from the last 350 to 395 m is only 0.08 °C. When the well depth is 160 m, the temperature change from 5 to 50 m is 0.61 °C and that from the last 270 to 315 m is only 0.15 °C. When the well depth is 120 m, the temperature change from 5 to 50 m is 0.56 °C and that from the last 190 to 235 m is 0.22 °C. When the well depth is 80 m, the temperature change from 5 to 50 m is 0.57 °C and that from the last 110 to 155 m is 0.35 °C. In addition, the deeper the well, the lower the overall temperature of the wall. As the fluid flows in the buried pipe, the temperature of the fluid decreases continuously, the temperature difference between the fluid and the soil decreases, and the heat transfer capacity decreases, and also the decreasing rate of the borehole wall temperature decreases along the pipe.

Figure 12 shows the water temperature distributions along the water flow direction when the well depths are 200, 160, 120, and

https://doi.org/10.1021/acsomega.3c01207
ACS Omega 2023, 8, 24964−24979

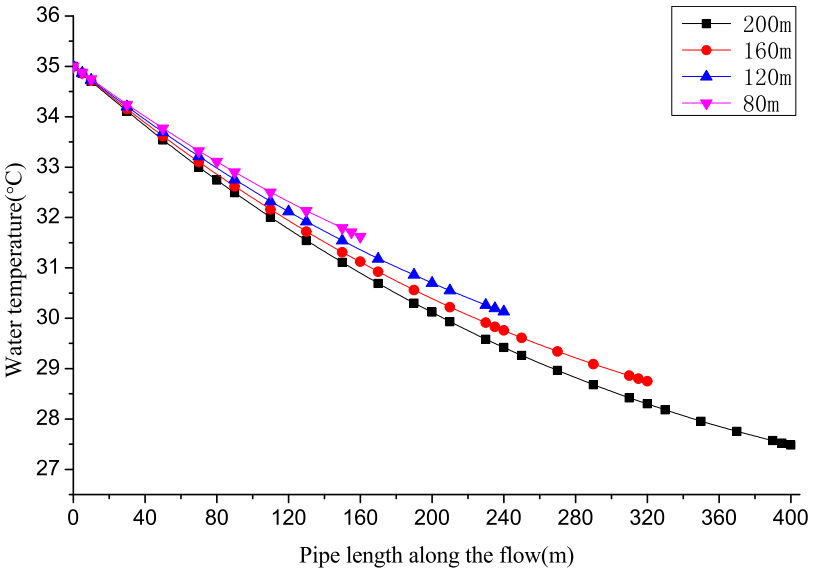

Figure 12. Water temperature distributions along the water flow direction after 24 h operation of buried pipes with different buried depths in summer.

80 m in summer. It can be seen that the water temperature decreases along the water flow direction and the temperature drop per unit length decreases gradually. When the well depth is 80 m, the temperature change per unit pipe length in the initial 5 m of the inlet pipe is 0.12 °C/m and that in the last 5 m of the outlet pipe is 0.09 °C/m, presenting a reduction of 25%. When the well depth is 120 m, the temperature change per unit pipe length in the initial 5 m of the inlet pipe is 0.13 °C/m and that in the last 5 m of the outlet pipe is 0.066 °C/m, which is a decrease of 49.2%. When the well depth is 160 m, the temperature change per unit pipe length in the initial 5 m of the inlet pipe is 0.14 °C/m and that in the last 5 m of the outlet pipe is 0.05 °C/m, which is a reduction of 64.3%. When the well depth is 200 m, the temperature change per unit pipe length in the initial 5 m of the inlet pipe is 0.14 °C/m and that in the last 5 m of the outlet pipe is 0.04 °C/m, which is a decrease of 71.4%. In addition, when the buried depths are 200, 160, 120, and 80 m, the temperature drops from 0 to 160 m along the water flow direction are 4.1, 3.88, 3.65, and 3.38 °C, respectively. It can be seen that a large buried depth of the buried pipe implies a large change in the water temperature along the same distance of the water flow during the same operation time. This is because a large buried depth implies less water circulation in the pipe, a small change in the surrounding soil temperature, and a large temperature difference between the circulating liquid and the soil. The heat exchange capacity is high, and the water temperature in the pipe changes sharply.

Table 4 summarizes the heat exchange ratios of the inlet and outlet pipe sections at different well depths in summer. It can be seen that a large well depth implies a large proportion of heat exchange in the inlet section and a small proportion of heat exchange in the outlet section. Specifically, a deep buried pipe implies a large concentration of heat exchange in the inlet section. Based on the above analysis, this can be attributed to the water temperature changing increasingly gradually along the water flow direction.

Figure 13 shows the variations in the temperature difference between the well wall and the fluid of the buried pipe heat exchangers along the water flow direction for different well depths under summer working conditions. It can be seen that the temperature difference between the well wall and the fluid

Table 4. Heat Exchange Ratios of Inlet and Outlet Pipe Sections of Buried Pipes for Different Well Depths in Summer

well depth (m)	temperature drop in the inlet section (°C)	temperature drop in the outlet section (°C)	heat exchange ratio of the inlet section (%)	heat exchange ratio of the outlet section (%)
80	1.89	1.48	55.9	43.8
120	2.88	1.98	59.1	40.7
160	3.88	2.36	62.1	37.8
200	4.88	2.63	64.9	35.0

decreases along the water flow direction. This temperature difference at a depth of 5 m in the water inlet section of the buried pipe at a well depth of 80 m is 6.03 °C, whereas that in the water outlet section is only 4.45 °C, which is a decrease of 26.2%. The temperature difference between the well wall and the fluid at a depth of 5 m in the water inlet section of the buried pipe at a well depth of 120 m is 7.09 °C. In comparison, that in the water outlet section is only 4.44 °C, a reduction of 37.4%. The temperature difference between the well wall and the fluid at a depth of 5 m in the water inlet section of the buried pipe at a well depth of 160 m is 7.24 °C. By contrast, that in the water outlet section is only 3.8 °C, which is a decrease of 47.5%. The temperature difference between the well wall and the fluid at a depth of 5 m in the water inlet section of the buried pipe at a well depth of 200 m is 7.39 °C. However, that in the water outlet section is only 3.15 °C, which is a reduction of 57.4%. A small temperature difference between the well wall and the fluid implies a poor heat exchange capacity between the circulating fluid and the soil. Therefore, the temperature of the circulating fluid changes increasingly gradually along the water flow direction. Simultaneously, it shows that a large well depth implies a large heat exchange proportion in the inlet section and a small heat exchange proportion in the outlet section.

3.3. Horizontal Temperature Distribution of the Borehole Wall and Water. Taking a buried pipe heat exchanger with a well depth of 80 m as an example, Figure 14 shows the horizontal temperature distribution of the inlet and outlet pipe segments and the surrounding soil at different depths when the inlet temperature is 35 °C in summer. The water

https://doi.org/10.1021/acsomega.3c01207
ACS Omega 2023, 8, 24964−24979

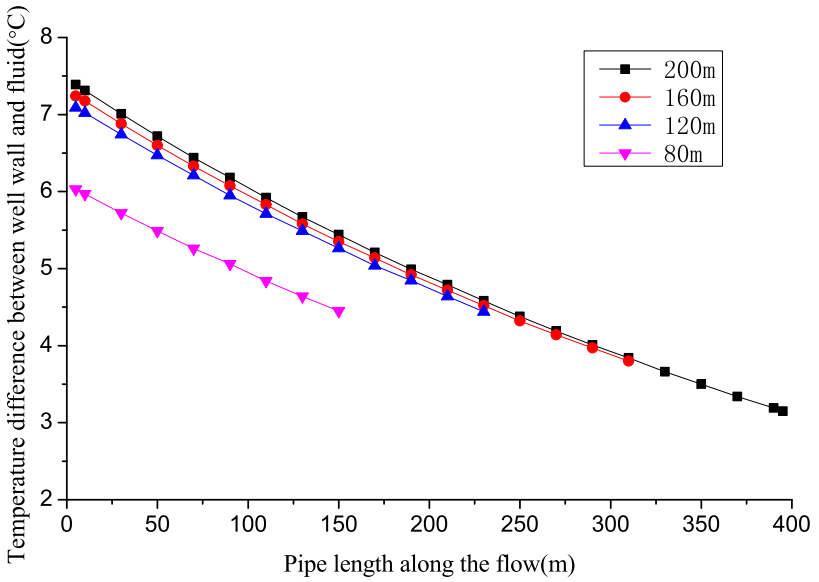

Figure 13. Variations in temperature difference between the well wall and the fluid along the water flow direction for different well depths.

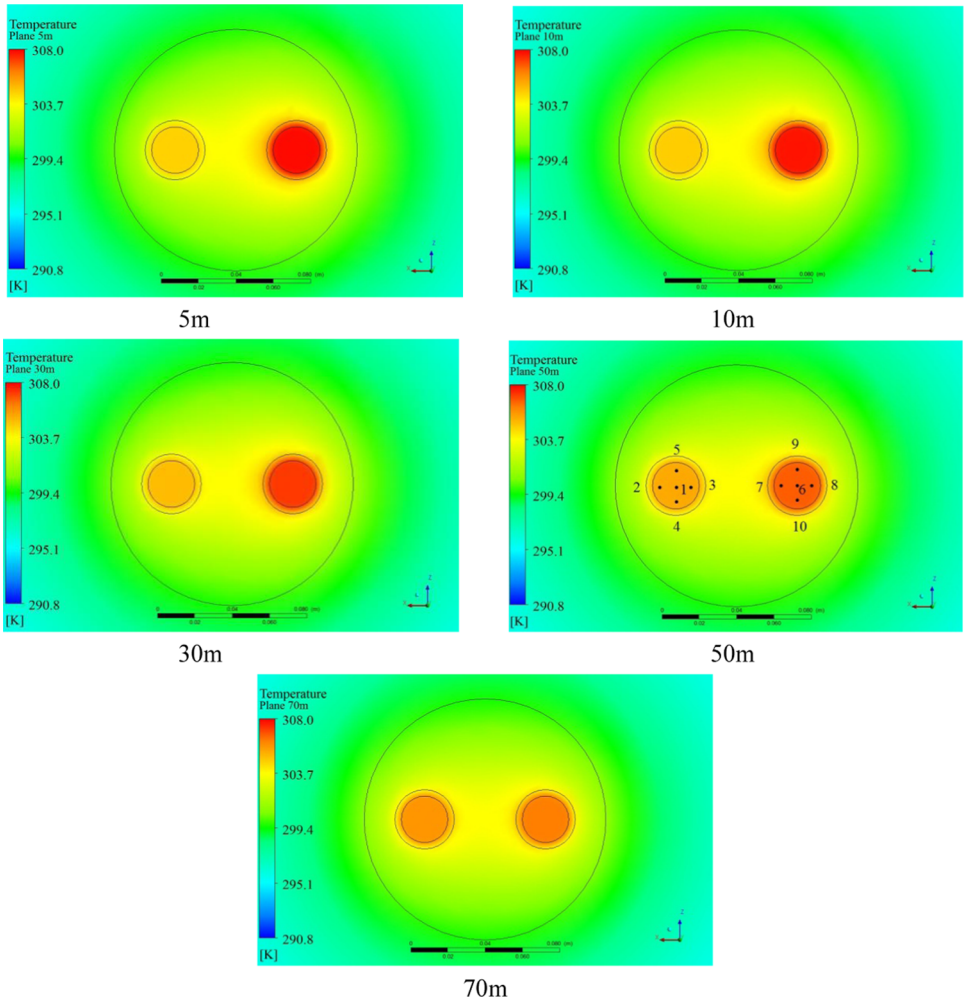

Figure 14. Horizontal water temperature distribution of the inlet and outlet pipe sections of the buried pipe heat exchanger at different depths in a well with depth 80 m.

temperature of the inlet section is higher than that of the outlet section, and the soil temperature around the inlet section is also higher. The smaller the depth, the greater the difference in the temperature of the horizontal surface of the inlet and outlet water because the water temperature decreases along the direction of the flow.

https://doi.org/10.1021/acsomega.3c01207
ACS Omega 2023, 8, 24964−24979

Table 5. Calculation Table of the Comprehensive Heat Transfer Coefficient

well depth (m)	heat transfer (W)	heat flux (W/m^2)	mean temperature of the borehole wall (°C)	mean temperature of the fluid (°C)	temperature difference between the well wall and fluid (°C)	heat transfer coefficient (W/(m^2 °C))
80	4156.8	127.29	28.01	33.31	5.3	24.02
120	5997.6	122.44	26.64	32.57	5.93	20.66
160	7694.4	117.81	26.07	31.88	5.81	20.29
200	9252	113.33	25.51	31.24	5.73	19.78

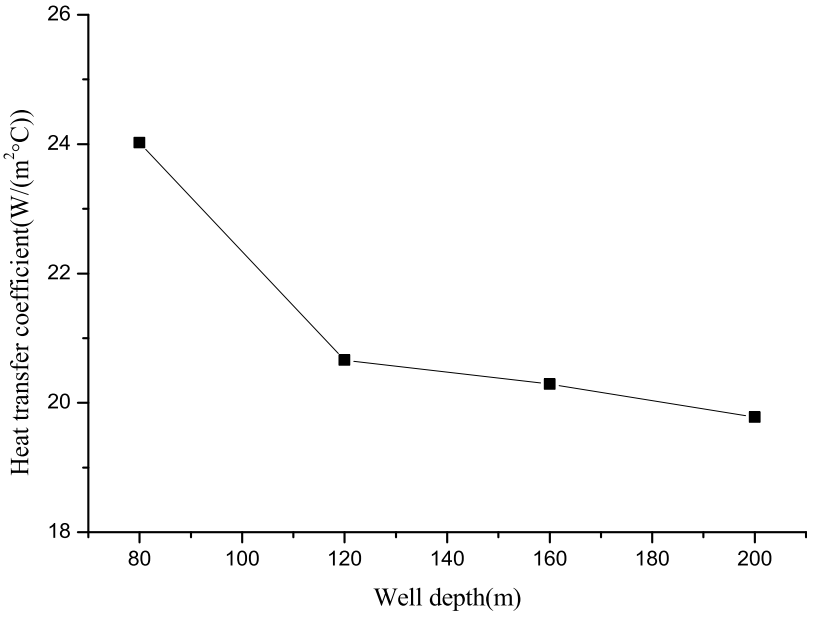

Figure 15. Comprehensive heat transfer coefficient of different well depths.

In addition, the horizontal temperature distribution of the inlet or outlet section at the same depth is inconsistent. Taking the water temperature distribution of the inlet and outlet sections at 50 m depth as an example, the temperature of the inlet section is 33.77 °C at point 6, 33.72 °C at point 7, 33.71 °C at point 8, 33.72 °C at point 9, and 33.72 °C at point 10; the temperature of the outlet section is 32.50 °C at point 1, 32.44 °C at point 2, 32.48 °C at point 3, 32.46 °C at point 4, and 32.45 °C at point 5. It can be seen that the temperature at the center of the water inlet and outlet sections is higher than that at the surrounding points, and the temperature at points 3 and 7 is higher. Because the inlet and outlet water pipe sections will transfer heat to the surrounding soil, and the inlet and outlet water pipe sections are close to each other, heat transfer will also occur between them, and it is difficult for heat to transfer to the surrounding soil, so that the temperature near points 3 and 7 is higher, while the temperature far away is lower.

3.4. Overall Heat Transfer Coefficient. The heat transfer of the buried pipe can be calculated as eq 9.

$$Q = mc_p(t_{in} - t_{out}) \tag{9}$$

where Q is the heat transfer of the buried pipe, W; and t_{in} and t_{out}, respectively, refer to the temperature of the inlet and outlet, °C.

The heat flux can be calculated as eq 10.

$$q = \frac{Q}{\pi dl} \tag{10}$$

where d is the inside diameter of the U-shaped pipe, m; and l is the length of the U-shaped pipe, m.

We define the overall heat transfer coefficient between the borehole wall and the fluid as eq 11.

$$K = \frac{q}{t_b - t_f} \tag{11}$$

where K is the heat transfer coefficient, W/(m^2 °C).

The overall heat transfer coefficient of different well depths was calculated as Table 5, and the results are shown in Figure 15. As can be seen from the figure, with the increase of well depth, the overall heat transfer coefficient between the well wall and the fluid shows a decreasing trend, and the decreasing degree becomes slower and slower. With the increase of well depth, the total heat transfer between the fluid in the buried pipe and the surrounding soil increased, but the heat transfer per unit area showed a decreasing trend. The average temperature difference between the fluid and the well wall first increased and then decreased with the change of well depth from 80 to 200 m. When the well depth was 80 m, the temperature difference was the smallest and the heat transfer per unit area was the largest, so the heat transfer coefficient was the largest.

4. VALIDITY OF THE BURIED PIPE SECTION

The validity of heat transfer of a buried pipe is used to determine its effective and invalid sections.[37] The energy efficiency, E, of a U-shaped buried tube heat exchanger is defined as the ratio of the actual heat exchange to the maximum theoretical heat exchange of the buried tube heat exchanger, and its expression is

https://doi.org/10.1021/acsomega.3c01207
ACS Omega 2023, 8, 24964−24979

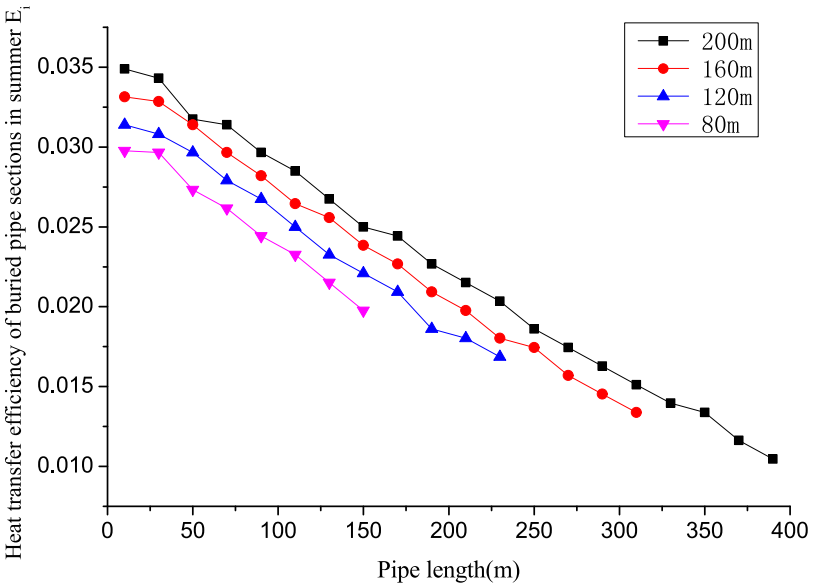

Figure 16. Heat transfer efficiency of buried pipe sections with different buried depths in summer.

Table 6. Simulation Conditions for Different Inlet Water Temperatures

working condition	season	inlet water temperature (°C)	current speed (m/s)	operation strategy	initial soil temperature (°C)
case a1	summer	40	0.6	continuous operation for 24 h	17.8
case a2		37			
case a3		35			
case a4		32			
case a5		30			

$$E = \frac{Q}{Q'} = \frac{mc_p(t_{in} - t_{out})}{mc_p(t_{in} - t_0)} = \frac{t_{in} - t_{out}}{t_{in} - t_0} \quad (12)$$

where t_{in}, t_{out}, and t_0 are the fluid inlet and outlet temperatures of the U-shaped buried pipe heat exchanger and the initial soil temperature, respectively, °C; and m is the mass flow of the fluid in the buried pipe, kg/s.

Under the condition of a certain flow, the heat exchange capacity between each section of the U-shaped buried pipe and the soil has an effect on the inlet and outlet temperature difference of the buried pipe. It can be considered that this temperature difference is gradually superimposed by the temperature difference of each small section. To analyze the influence of each section on the overall heat transfer efficiency of the buried pipe, the buried pipe heat exchanger can be arbitrarily divided into n sections, and the inlet and outlet temperature difference of the entire buried pipe can be expressed as

$$\Delta t = t_{in} - t_{out} = \Delta t_1 + \Delta t_2 + L + \Delta t_n \quad (13)$$

where Δt_i $(i = 1, 2, L, n)$ represents the fluid temperature difference in a section, °C.

Dividing both sides of the above equation by $t_{in} - t_0$, we obtain

$$\frac{\Delta t}{t_{in} - t_0} = \frac{t_{in} - t_{out}}{t_{in} - t_0} = \frac{\Delta t_1}{t_{in} - t_0} + \frac{\Delta t_2}{t_{in} - t_0} + L + \frac{\Delta t_n}{t_{in} - t_0} \quad (14)$$

Referring to the definition of the energy validity, E, E_i is called the heat exchange energy validity of the buried pipe section and is expressed as

$$E_i = \frac{\Delta t_i}{t_{in} - t_0} \ (i = 1, 2, L, n) \quad (15)$$

The total energy validity, e, of the buried pipe is the sum of all section heat exchange validities, i.e., $E = \sum_{i=1}^{n} E_i$.

Figure 16 shows the heat transfer efficiencies of buried tube heat exchangers for different depths in summer. Different from the well wall temperature and the water temperature in the pipe, the change in the heat transfer efficiency along the water flow direction is not a smooth curve; instead, it shows an overall decreasing trend.

When the well depth is 200 m, the heat exchange efficiency of the initial 0−10 m pipe section is 0.0349, whereas the energy efficiency of the 390−400 m pipe section is reduced to 0.01047, which is only 30% of the former. When the well depth is 160 m, the heat exchange efficiency of the initial 0−10 m pipe section is 0.0331, whereas the energy efficiency of the 310−320 m pipe section is reduced to 0.01337, which is only 40.3% of the former. When the well depth is 120 m, the heat exchange efficiency of the initial 0−10 m pipe section is 0.0314, whereas the energy efficiency of the final 230−240 m pipe section is 0.0169, which is 53.7% of the former. When the well depth is 80 m, the heat transfer efficiency of the initial 0−10 m pipe section is 0.02976, whereas the energy efficiency of the last 150−160 m pipe section is 0.01977, reaching 66.4% of the former.

5. ANALYSIS OF OTHER INFLUENCING FACTORS

Taking a buried pipe heat exchanger with a well depth of 80 m as an example, the influences of the buried pipe inlet temperature, soil temperature, and circulating liquid velocity on heat exchange performance were analyzed.

https://doi.org/10.1021/acsomega.3c01207
ACS Omega 2023, 8, 24964−24979

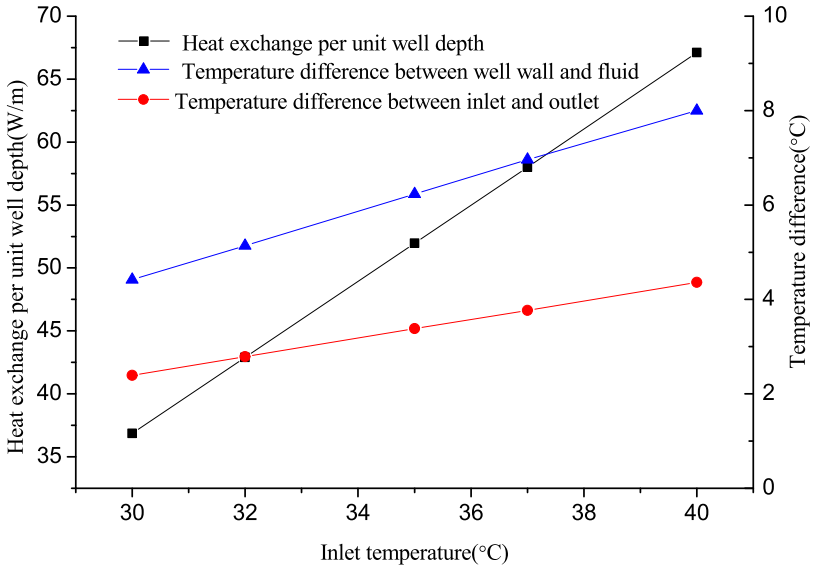

Figure 17. Comparison of heat exchanges and temperature differences for different inlet temperatures.

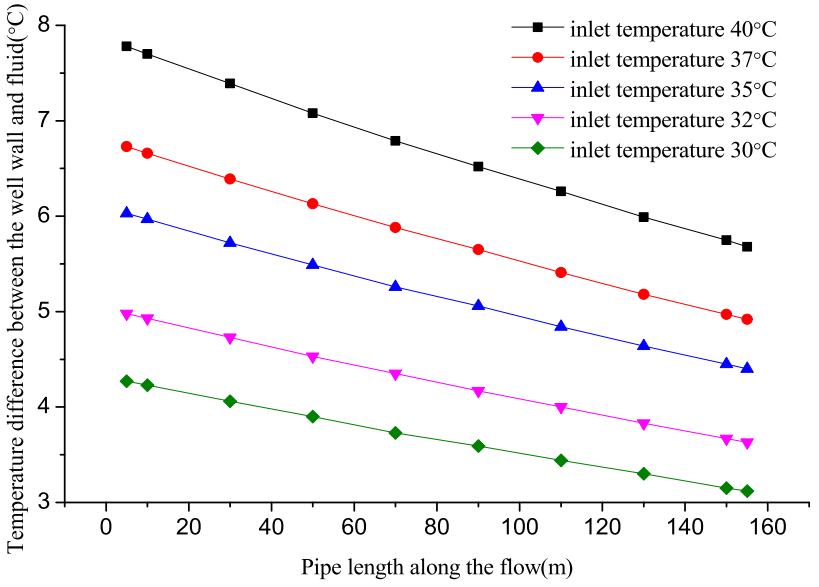

Figure 18. Variations in temperature difference between the well wall and the fluid along the water flow direction for different inlet temperatures.

5.1. Inlet Temperature of the Buried Pipe. In this section, the analysis and comparison of single U-shaped buried pipe heat exchangers with inlet temperatures of 40, 37, 35, 32, and 30 °C are presented. The specific simulation conditions are listed in Table 6.

(1) Heat exchange comparison

Figure 17 shows the comparison of the heat transfer performance of buried pipes for different inlet temperatures after 24 h operation. It can be seen that, with the increase of inlet temperature in the summer, the temperature difference between the well wall and the fluid increases, the heat transfer capacity increases, the temperature difference between the inlet and outlet water increases, and the heat transfer per unit well depth increases. When the inlet temperature is 30 °C, the heat exchange per unit well depth is 36.85 W/m after 24 h operation, while when the inlet temperature reaches 40 °C, the heat exchange is 67.1 W/m, which is 82.1% higher than that at 30 °C. However, the increase of the water inlet temperature will lead to an increase of the condensing temperature of the heat pump and a decrease of the efficiency of the heat pump. Moreover, in actual operation, the water inlet temperature of the buried pipe will change with the change of indoor load. When the indoor load is too large or the number of buried pipes is insufficient, the outlet temperature of the heat pump, namely, the inlet temperature of the buried pipe, will rise.

(2) Temperature difference between well wall and fluid

Figure 18 shows the temperature difference between the well wall and the fluid along the water flow direction for different inlet temperatures. It can be seen that the higher the inlet temperature is, the greater the temperature difference between the well wall and the water is. When the inlet temperature is 40 °C, the temperature difference along the flow direction is 7.78 °C at 5 m and 5.68 °C at 155 m, which decreases by 26.99%. When the inlet temperature is 35 °C, the temperature difference along the flow direction is 6.03 °C at 5 m and 4.4 °C at 155 m, which decreases by 27.03%. When the inlet temperature is 30 °C, the

https://doi.org/10.1021/acsomega.3c01207
ACS Omega 2023, 8, 24964−24979

Table 7. Simulation Conditions for Different Soil Temperatures

working condition	season	inlet water temperature (°C)	current speed (m/s)	operation strategy	initial soil temperature (°C)
case a3	summer	35	0.6	continuous operation for 24 h	17.8
case b1					19
case b2					21
case b3					23
case b4					25

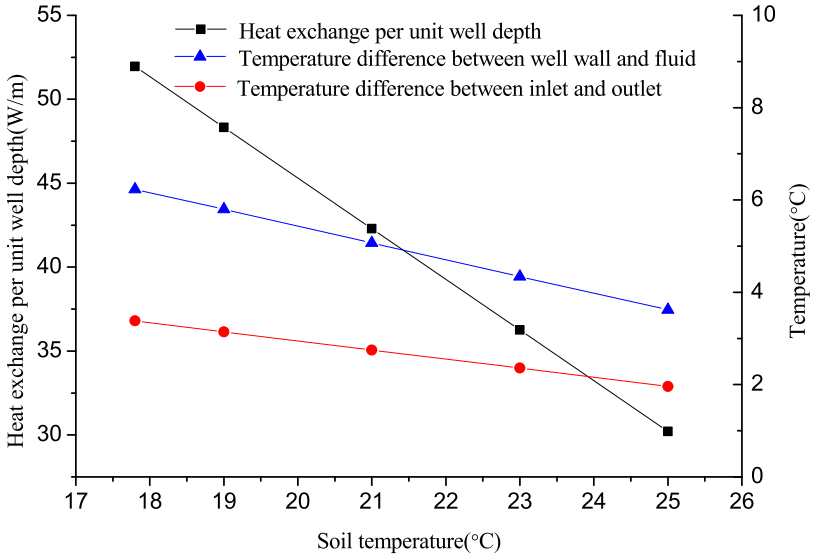

Figure 19. Comparison of the heat transfer performance of buried pipe heat exchangers with different soil temperatures in summer.

Table 8. Simulation Conditions for Different Current Speeds

working condition	season	current speed (m/s)	operation strategy	inlet water temperature (°C)	initial soil temperature (°C)
case c1	summer	0.3	continuous operation for 24 h	35	17.8
case a3		0.6			
case c2		0.9			
case c3		1.2			

temperature difference along the flow direction is 4.27 °C at 5 m and 3.12 °C at 155 m, which decreases by 26.93%. It can be seen that when the inlet temperature is different, the temperature difference between the fluid and the well wall decreases by almost the same degree along the water flow direction.

5.2. Soil Temperature. In this section, the analysis and comparison of single U-shaped buried pipe heat exchangers with soil temperatures of 17.8, 19, 21, 23, and 25 °C are presented. The specific simulation conditions are listed in Table 7.

Figure 19 shows the comparison of the heat exchange performance of the buried pipe heat exchanger in summer with different soil temperatures. It can be seen that the higher the soil temperature, the smaller the temperature difference between the well wall and the fluid, the lower the heat exchange performance of the buried pipe, and the smaller the temperature difference between the inlet and outlet water, the lower the heat exchange per unit well depth. When the soil temperature increased from 17.8 to 25 °C, heat transfer per unit well depth decreased from 51.96 to 30.21 W/m by 41.8%.

5.3. Current Speed. In this section, the analysis and comparison of single U-shaped buried pipe heat exchangers with current speeds of 0.3, 0.6, 0.9, and 1.2 m/s are presented. The specific simulation conditions are listed in Table 8.

Table 9 shows the well wall temperature, the inlet and outlet water temperature difference, and the heat transfer rate inside and outside the pipe during 24 h operation of the buried pipe at different flow rates. It can be seen that the higher the flow velocity, the less sufficient the heat transfer between the fluid and soil. When the inlet temperature is stable, the higher the outlet temperature, the higher the average fluid temperature, and the higher the heat transfer rate from the buried pipe to the well wall, the higher the temperature of the well wall. Although the high current speed leads to insufficient heat transfer with soil, which reduces the temperature difference between the inlet and the outlet of the buried pipe, the total heat exchange still increases with the increase of the current speed. When the current speed is 0.3 m/s, the temperature difference between the inlet and the outlet reaches 6.04 °C. When the current speed increases to 1.2

Table 9. Comparison of the Heat Transfer Performance of Buried Pipes with Different Current Speeds

current speed (m/s)	well wall temperature (°C)	heat exchange outside of the pipe (W/m)	temperature difference between the inlet and outlet (°C)	heat exchange inside of the pipe (W/m)	heat exchange difference between the inside and outside of the pipe (W/m)
0.3	25.83	38.99	6.04	46.42	7.43
0.6	26.94	43.09	3.38	51.96	8.87
0.9	27.34	44.48	2.33	53.86	9.38
1.2	27.55	45.18	1.78	54.83	9.65

https://doi.org/10.1021/acsomega.3c01207
ACS Omega 2023, 8, 24964−24979

m/s, the temperature difference between the inlet and the outlet is only 1.78 °C, which decreases by 70.5%. However, the heat exchange at 1.2 m/s is 54.83 W/m, 18.1% higher than 46.42 W/m at 0.3 m/s, and the well wall temperature is 1.72 °C higher than that at 0.3 m/s. Therefore, increasing the current speed increases the heat transfer rate of the fluid in the pipe, but it causes the wall temperature to rise even higher. When the current speeds are 0.3, 0.6, 0.9, and 1.2 m/s, respectively, the well wall temperatures increase by 8.03, 9.14, 9.54, and 9.75 °C compared with the initial temperature.

6. CONCLUSIONS

(1) In summer, as the buried depth of a buried pipe increases, the temperature difference between the inlet and the outlet increases, whereas the heat exchange per unit well depth decreases. Therefore, a large buried depth is ineffective. When the well depths are 200, 160, 120, and 80 m, the heat exchanges per unit well depth in summer after 24 h operation are 46.26, 48.09, 49.98, and 51.96 W/m, respectively.

(2) In summer, the wellbore temperature decreases along the flow direction, and the temperature changes increasingly gradually. Along the flow direction, the water temperature in the U-shaped pipe decreases gradually, and similar to the wellbore temperature, the water temperature changes increasingly gradually. The heat exchange is mainly concentrated in the inlet section. With the increase in the buried pipe depth, the proportion of heat exchange in the inlet section to the total heat exchange increases.

(3) In summer, the temperature difference between the well wall and the fluid decreases along the water flow direction. When the depth is the same, the temperature differences at a depth of 5 m in the outlet section decrease by 26.3, 37.3, 47.7, and 57.2% compared to that in the inlet section when the well depths are 80, 120, 160, and 200 m, respectively.

(4) The concept of section heat transfer efficiency is introduced to analyze the energy efficiencies of the heat exchange sections of buried tube heat exchangers with buried depths of 200, 160, 120, and 80, respectively. In summer, when the well depths are 200, 160, 120, and 80 m, the last 10 m pipe sections have 30, 40.3, 53.7, and 66.4% of the heat exchange efficiency of the initial 10 m pipe section, respectively.

(5) With the increase of well depth, the comprehensive heat transfer coefficient between the well wall and the fluid showed a decreasing trend, and it decreased more and more slowly. The comprehensive heat transfer coefficient reached the maximum at 80 m depth, which was 24.02 W/m^{2}K.

(6) To obtain a reasonable effective well depth of a single U-shaped vertical buried pipe, it is necessary to comprehensively consider the heat exchange per unit well depth, the temperature difference between the well wall and the fluid, and the energy efficiency of the buried pipe section. Moreover, this analysis should be conducted in combination with economic factors.

(7) The other factors affecting the buried pipe heat exchanger are analyzed and compared. For the inlet temperature, the higher the inlet temperature, the greater the heat exchange. For soil temperature, the higher the soil temperature, the smaller the heat exchange. For the current speed, the higher the flow velocity is, the greater the heat exchange.

AUTHOR INFORMATION

Corresponding Author

Rui Zhang − *Shandong Institute of Petroleum and Chemical Technology, Dongying 257000 Shandong, China*; Email: lotus0215@163.com

Author

Yanping Xin − *Shandong Institute of Petroleum and Chemical Technology, Dongying 257000 Shandong, China*

Complete contact information is available at: https://pubs.acs.org/10.1021/acsomega.3c01207

Funding

This work was supported by the Youth Innovation Team Science and Technology Development Program of Shandong Province Higher Educational Institutions (2019KJA024) and the Science Development Funding Program of Dongying of China(DJ2020009).

Notes

The authors declare no competing financial interest.

REFERENCES

(1) Jin, G.; Li, Z.; Zhang, K.; Zhao, W.; Wu, M.; Guo, S. Regional thermal efficiency analysis of buried pipe groups in layered rock and soil. *J. Sol. Energy* **2021**, *42*, 487−492.

(2) Yu, B.; Hao, N.; Jin, G.; Guo, S.; Chen, Z. Study on heat transfer characteristics of vertical buried tube heat exchanger considering soil stratification. *Soil Bull.* **2020**, *51*, 315−324.

(3) Min, J. Study on Factors Affecting the Performance of Ground Pipe Heat Exchanger of Ground Source Heat Pump, Master's Thesis; Anhui Architecture University: Anhui, 2021.

(4) Chwieduk, M. New global thermal numerical model of vertical U-tube ground heat exchanger. *Renewable Energy* **2021**, *168*, 343−352.

(5) Lu, W. Effect of geotechnical vertical temperature gradient on the performance of buried tube heat exchanger. *Gas Heat* **2020**, *40*, 23−27.

(6) Chen, Z. Study on heat transfer performance of buried tube heat exchanger of ground source heat pump. *J. Vac. Sci. Technol.* **2020**, *40*, 495−498.

(7) Xu, S.; Liu, Y.; Yuan, D. Research status and Prospect of enhanced heat transfer based on buried heat exchanger. *Fluid Mach.* **2019**, *47*, 68−75.

(8) Guo, M.; Diao, N.; Zhu, K.; Fang, Z. Design and operation countermeasures of geothermal heat exchanger in areas with unbalanced cooling and heating load. *J. Beijing Univ. Technol.* **2019**, *45*, 88−94.

(9) He, Z.; Yu, M.; Mao, Y.; Fang, Z. Heat transfer analysis of buried tube heat exchanger based on adaptive load distribution. *J. Eng. Thermophys.* **2020**, *41*, 2044−2051.

(10) Cai, Y. Study on Influencing Factors of Heat Transfer Capacity of Vertical Buried Tube Heat Exchanger, Master's Thesis; China University of Geosciences (Beijing): Beijing, 2020.

(11) Yang, W.; Xu, R.; Yang, J.; Chen, S. Numerical simulation and experimental verification of thermal response characteristics of buried pipe heat exchanger backfilled with phase change materials. *Fluid Mach.* **2019**, *47*, 72−79.

(12) Shang, S.; Pan, X.; Xu, Y.; Fang, Y. Simulation of the effect of soil specific heat capacity on soil temperature around buried pipe heat exchanger. *J. Shenyang Archit. Univ.* **2019**, *35*, 379−384.

(13) Wang, C. Study on Enhanced Heat Transfer Mechanism and Characteristics of Buried Tube Heat Exchanger, Master's Thesis; Zhejiang University of Technology: Zhejiang, 2018.

(14) Bao, Y. Numerical Simulation Analysis of Heat Transfer Performance of Vertical Double U-Shaped Buried Tube Heat

Exchanger, Master's Thesis; Hubei University of technology: Hubei, 2018.
(15) Tang, P.; Ling, S.; Yang, Y.; Cui, Q.; Gong, Y. Measurement and analysis of buried tube heat exchangers in Nanjing. *J. Sol. Energy* **2017**, *38*, 378−385.
(16) Diao, N.; Fang, Z. *Buried Pipe Ground Source Heat Pump Technology*; Higher Education Press: Beijing, 2006.
(17) Wang, Y. Performance of Ground Source Heat Pump under Dynamic Load, Doctoral Thesis; Chongqing University: Chongqing, 2006.
(18) Cai, Y.; Zhang, H.; Chen, S.; Fu, Y.; Huang, S. Experimental study on ground source heat pump heating with different buried heat exchangers in winter. *J. Hunan Univ.* **2009**, *36*, 22−26.
(19) Jin, G.; Zhang, X.; Wu, M.; Tian, R.; Bi, W.; Wang, W. Evaluation and analysis of thermal short circuit of buried pipe based on unbalance coefficient. *Fluid Mach.* **2016**, *44*, 75−82.
(20) Li, C.; Jiang, C.; Yang, R.; Liu, J.; Yang, C.; Guan, Y. Effects of buried depth and connecting pipe length on heat transfer of U-shaped deep buried pipe. *J. Sol. Energy* **2021**, *42*, 490−495.
(21) Li, Z.; Du, Z. Influence of groundwater seepage on buried depth of single U-shaped buried pipe. *Sci., Technol. Eng.* **2021**, *21*, 9068−9073.
(22) Lin, Z.; Wang, Z.; Wang, Y. Study on Optimization of buried depth of vertical buried tube heat exchanger of ground source heat pump. *J. Kunming Univ. Technol.* **2020**, *45*, 74−79.
(23) Li, M.; Li, X.; Wang, B.; Zhao, P.; Dong, S.; Liu, A. Study on heat transfer characteristics of buried pipes in geological structure stratification. *J. Sol. Energy* **2020**, *41*, 290−294.
(24) Deng, J.; Wang, J.; Zheng, J. Heat transfer performance analysis of buried tube heat exchangers with different pipe diameters and buried depths. *J. Sol. Energy* **2021**, *42*, 416−421.
(25) Yang, L.; Zhang, B.; Klemeš, J. J.; Liu, J.; Song, M. Y.; Wang, J. Effect of buried depth on thermal performance of a vertical U-tube underground heat exchanger. *Open Phys.* **2021**, *19*, 327−330.
(26) Zhang, C.; Wang, X.; Sun, P.; Kong, X.; Sun, S. Effect of depth and fluid flow rate on estimate for borehole thermal resistance of single U-pipe borehole heat exchanger. *Renewable Energy* **2020**, *147*, 2399−2408.
(27) Chen, S.; Mao, J.; Chen, F.; Hou, P.; Li, Y. Development of ANN model for depth prediction of vertical ground heat exchanger. *Int. J. Heat Mass Transfer* **2018**, *117*, 617−626.
(28) Song, W.; Zheng, T.; Wang, M. Theoretical Study on Arrangement Depth of U-Tube Heat Exchanger under Building Foundation. *Procedia Eng.* **2017**, *205*, 3170−3177.
(29) Honda, H.; Wijayantab, A. T.; Takataa, N. Condensation of R407C in a horizontal microfin tube. *Int. J. Refrig.* **2005**, *28*, 203−211.
(30) Koji, E.; Masaharu, O.; Tomio, O.; Budi, K.; Agung, T. W. Water flow boiling heat transfer in vertical minichannel. *Exp. Therm. Fluid Sci.* **2020**, *117*, 110−147.
(31) Qi, C.; Wang, G.; Yang, L.; Wan, Y.; Rao, Z. Two-phase lattice Boltzmann simulation of the effects of base fluid and nanoparticle size on natural convection heat transfer of nanofluid. *Int. J. Heat Mass Transfer* **2017**, *105*, 664−672.
(32) Wang, Y.; Qi, C.; Ding, Z.; Tu, J.; Zhao, R. Numerical simulation of flow and heat transfer characteristics of nanofluids in built-in porous twisted tape tube. *Powder Technol.* **2021**, *392*, 570−586.
(33) Tu, J.; Qi, C.; Li, K.; Tang, Z. Numerical analysis of flow and heat characteristic around micro-ribbed tube in heat exchanger system. *Powder Technol.* **2022**, *395*, 562−583.
(34) Wang, C.; Qi, C.; Han, D.; Wang, Y.; Sun, L. Effects of modified surface on flow and heat transfer of heat pipe. *Eur. Phys. J. Plus* **2022**, *137*, No. 318.
(35) Kazemi-Beydokhti, A.; Meyghani, N.; Samadi, M.; Hajiabadi, S. H. Surface modification of carbon nanotube: Effects on pulsating heat pipe heat transfer. *Chem. Eng. Res. Des.* **2019**, *152*, 30−37.
(36) Leu, T.-S.; Wu, C.-H. Experimental studies of surface modified oscillating heat pipes. *Heat Mass Transfer* **2017**, *53*, 3329−3340.
(37) Yu, Z.; Hu, P.; Xu, Y.; Yuan, X.; Ma, Y. Design of buried depth of vertical buried pipe based on heat exchange efficiency. *Heat., Vent., Air-Cond. Refrig.* **2009**, *39*, 98−101.

https://doi.org/10.1021/acsomega.3c01207
ACS Omega 2023, 8, 24964−24979